Proceedings of the World Congress on Engineering and Computer Science 2010 Vol II
WCECS 2010, October 20-22, 2010, San Francisco, USA

Modeling and Control of a DC-DC Multilevel Boost Converter

J. C. Mayo-Maldonado, R. Salas-Cabrera, H. Cisneros-Villegas, M. Gomez-Garcia, E. N. Salas-Cabrera, R. Castillo-Gutierrez and O. Ruiz-Martinez

***Abstract*— This paper proposes a full order nonlinear dynamic model for a DC-DC Multilevel Boost Converter (MBC). This model is based on the equivalent circuits that depend on the commutation states of the converter. A reduced order nonlinear model to approximate the dynamics of the MBC containing any number of levels is also obtained. In addition, an input-output feedback linearization controller is derived and implemented. The stability of the closed loop system is analyzed. A Linux-based real-time software is employed for obtaining the experimental results of the closed loop system.**

***Keywords*—Current control, Circuit modeling, Nonlinear systems, State space methods.**

I. Introduction

During the last decades, increased attention has been given to renewable energy generation systems. There are plenty of issues to be analyzed and solved in this area. For example, the low DC voltage provided by renewable energy sources has to be boosted before being inverted and connected to the grid. Addressing this particular problem, several transformer-less DC-DC converters with high efficiency and high boost ratios have emerged. Some of these converters have high complexity compared to a conventional single switch converter [1]-[5].

The DC-DC Multilevel Boost Converter (MBC) studied in this paper is a power electronics device that was recently proposed [6-7]. The MBC presents several advantages in comparison to the conventional boost converter and other topologies. Figure 1 shows the MBC discussed in this paper. Some of the advantages are fewer components, self voltage balancing [8] and high voltage gain without using an extreme duty ratio and without employing a transformer. In addition, more levels can be added without modifying the main circuit [6].

There are several contributions in this paper. Since the MBC is a recently proposed topology its dynamic model is not available in the literature. We propose both a full order nonlinear dynamic model and a reduced order nonlinear dynamic model for the MBC. In addition, a new controller for the MBC is obtained by utilizing the differential geometry theory [13]. In particular, input-output feedback linearization is employed to control the inductor current. In our approach, the output voltage is indirectly controlled by defining a reference for the inductor current. The controller is derived by using the proposed reduced order model. The stability of the zero dynamics of the closed loop system is analyzed. Experimental results of the closed loop implementation are also presented.

Previous works present different models for other boost converters. In [9] authors propose both nonlinear and average linear models for a quadratic boost converter. In [10], authors propose a single-input-single-output model for an AC-DC boost converter; the model is similar to the model of the conventional DC-DC boost converter.

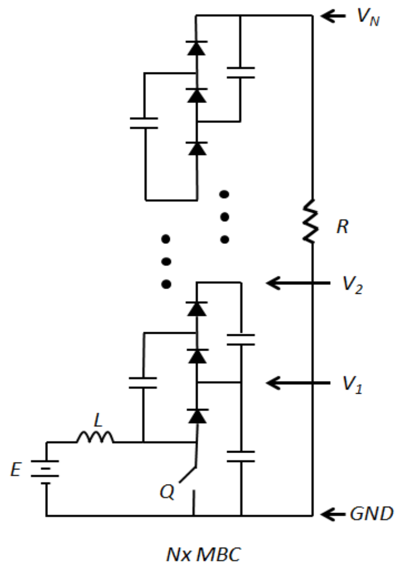

Fig. 1. Electrical diagram of the Nx Multilevel Boost Converter.

Different control techniques for power electronics devices can be found in the literature. In [11], a wide series of control techniques are presented for well known power electronics converters, including the conventional DC-DC boost converter. In [5], authors present experimental results of the implementation of a current-mode control for the quadratic boost converter. In [12], authors present some current controllers for three-phase boost rectifiers.

Before proceeding with the modeling an important feature of the MBC will be studied.

II. Voltage Balancing

One of the features of the MBC is voltage balancing [8]. In other words, the voltage across every capacitor at the output of the MBC tends to be equal. Even during transient

Authors are with the Instituto Tecnologico de Ciudad Madero, Av. 1o Mayo S/N Col. Los Mangos Ciudad Madero, Mexico (email jcarlos_mayo@hotmail.com).

This work was supported in part by the Instituto Tecnologico de Cd. Madero, the Fondo Mixto de Fomento a la Investigacion Cientifica y Tecnologica COTACyT-Gobierno del Estado de Tamaulipas and the DGEST under project No. 3607.10-P "Sintesis e implementacion de un emulador de un aerogenerador en tiempo real".

ISBN: 978-988-18210-0-3
ISSN: 2078-0958 (Print); ISSN: 2078-0966 (Online)

conditions these voltages are similar. In order to illustrate this feature the 3x MBC will be considered. It is clear that the electrical diagram of the 3x MBC shown in Fig. 2 is a particular case of the Nx MBC in Fig. 1. The transient behavior of the voltages across the capacitors at the output are depicted in Fig. 3. These traces were obtained by using the Synopsys Saber software and employing the electrical diagram of the 3x MBC.

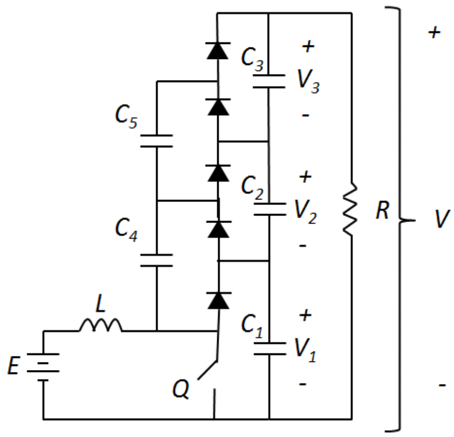

Fig. 2. Electrical diagram of the 3x MBC.

Average voltages in C_2 and C_3 (V_2 and V_3 respectively) are identical, while the average voltage in C_1 (V_1) is similar, see Fig. 3. This behavior is still present in a MBC having any number of levels (any number of capacitors) at the output.

On the other hand, it is important to note that the MBC was designed for increasing the gain of the voltage by adding capacitors at the output [6-7]. In our reduced order modeling approach, the main interest will be focused on defining the dynamics of an approximate output voltage rather than defining the dynamics of the voltage across every capacitor at the output.

The output voltage, during transient and steady state conditions, is defined as the sum of the voltages across the capacitors at the output of the MBC. Fig. 3 also depicts the transient behavior of the output voltage divided by the number of levels at the output (V/N). The notation for the number of capacitors at the output of the MBC is N. It is clear that V/N is similar to the voltage across each capacitor at the output.

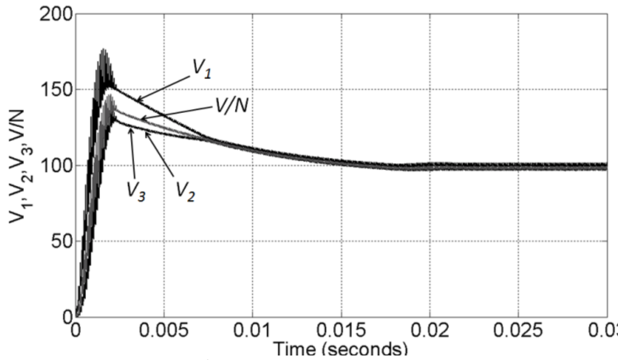

Fig. 3. Transient traces of the voltages across the capacitors at the output of the MBC and the dynamics of V/N.

III. Modeling of The DC-DC Multilevel Boost Converter

In this section we will be presenting both the full order nonlinear dynamic model and a reduced order nonlinear dynamic model for the MBC. The proposed models are obtained from the equivalent circuits depending on the commutation states of the converter. The derived reduced order model is able to define an approximate dynamics for the MBC containing any number of levels without modifying the order of the dynamic model. This feature provides several advantages for control design and implementation.

A. *Full Order Modeling*

Let us consider the electrical diagram in Fig. 4 that depicts a 2x MBC. This converter has 2 capacitors at the output (C_1 and C_2). For this particular converter the number N is equal to 2. In this section V_3 is a notation related to a voltage across a capacitor that is not at the output of the MBC.

In addition, let us define an input $u = \{1,0\}$ associated with the commutation states of the switch.

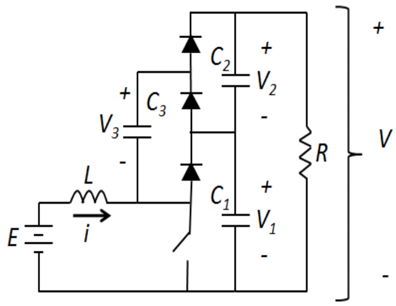

Fig. 4. Electrical diagram for a 2x DC-DC Multilevel Boost Converter.

Figure 5 shows the equivalent circuit for a 2x MBC when the switch is closed, this is $u = 1$.

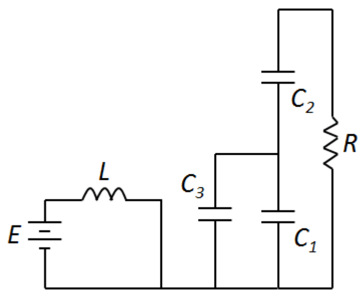

Fig. 5. Equivalent circuit for a 2x DC-DC Multilevel Boost Converter when the switch is closed.

Equations (1)-(4) represent the dynamics related to the inductor and the $N+1$ capacitors of a 2x MBC when the switch is closed.

$$\frac{d}{dt}i = \frac{1}{L}E \tag{1}$$

ISBN: 978-988-18210-0-3
ISSN: 2078-0958 (Print); ISSN: 2078-0966 (Online)

$$\frac{d}{dt}V_1 = -\frac{1}{(C_1+C_3)R}V_1 - \frac{1}{(C_1+C_3)R}V_2 - \lambda_1(t) \tag{2}$$

$$\frac{d}{dt}V_2 = -\frac{1}{(C_2R)}V_1 - \frac{1}{(C_2R)}V_2 \tag{3}$$

$$\frac{d}{dt}V_3 = -\frac{1}{(C_1+C_3)R}V_1 - \frac{1}{(C_1+C_3)R}V_2 + \lambda_1(t) \tag{4}$$

In equation (2) and (4), function $\lambda_1(t)$ represents a very fast transient that occurs when capacitors C_1 and C_3 are connected in parallel (see Fig. 5). Function $\lambda_1(t)$ is given by the following equation

$$\lambda_1(t) = \frac{V_1 - V_3}{R_G C_1}$$

where R_G is a very small resistance. If it is assumed that the resistances of the diodes and capacitors are neglected then the value of R_G tends to be zero.

As voltages across capacitors C_1 and C_3 tend to be equal, the function $\lambda_1(t)$ approximates to zero. Therefore, $\lambda_1(t)$ defines the dynamics in which C_3 obtains energy from C_1 when the switch is closed. The rest of the terms of the state equations (1)-(4) produce slower transients.

Figure 6 shows the equivalent circuit when the switch is opened, this is $u = 0$.

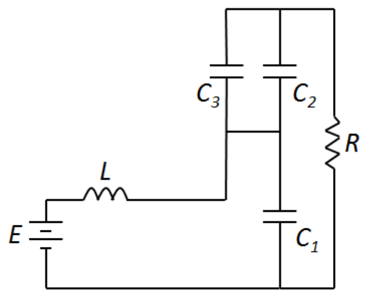

Fig. 6. Equivalent circuit for a 2x DC-DC Multilevel Boost Converter when the switch is opened.

Equations (5)-(8) represent the dynamics of the converter when the switch is opened.

$$\frac{d}{dt}i = -\frac{\mathrm{V}_1}{\mathrm{L}} + \frac{1}{L}E \tag{5}$$

$$\frac{d}{dt}V_1 = \frac{\mathrm{i}}{C_1} - \frac{1}{(C_1R)}V_1 - \frac{1}{(C_1R)}V_2 \tag{6}$$

$$\frac{d}{dt}V_2 = -\frac{1}{(C_1+C_2)R}V_1 - \frac{1}{(C_1+C_2)R}V_2 + \lambda_2(t) \tag{7}$$

$$\frac{d}{dt}V_3 = -\frac{1}{(C_1+C_3)R}V_1 - \frac{1}{(C_1+C_3)R}V_2 - \lambda_2(t) \tag{8}$$

State equations associated with the voltages across capacitors C_2 and C_3 have a term denoted by $\lambda_2(t)$. This function defines a transient similar to the one defined by $\lambda_1(t)$ when capacitors C_1 and C_3 were connected in parallel. The function $\lambda_2(t)$ can be expressed as

$$\lambda_2(t) = \frac{V_3 - V_2}{R_G C_3}$$

Therefore, when the switch is closed, C_3 obtains energy from C_1, this task is represented by $\lambda_1(t)$. On the other hand, when the switch is opened, C_3 transfers energy to C_2, this is represented by $\lambda_2(t)$. It is possible to conclude that capacitor C_3 works as the circuital vehicle that transports energy from capacitor C_1 to capacitor C_2. In general, there are always $N-1$ capacitors transferring energy to the capacitors at the output.

Let us consider the inductor current as the output of the dynamic system, this is

$$h(x) = [1\ \ 0\ \ 0\ \ 0][\,i\ \ V_1\ \ V_2\ \ V_3\,]^T = i \tag{9}$$

The selection of this variable as an output will be explained as the controller is derived in Section IV.

The full order nonlinear dynamic model is composed by state equations (1)-(8) and the output equation in (9). When more levels are added to the circuit (see Fig. 1), the number of equations increases as well, however the system has always the same circuital structure. It is clear that the dimension of the state space increases when more capacitors are added. However, it is possible to make use of the voltage balancing feature of the MBC and obtain a reduced order model. This model should be able to approximate the dynamics of the system having any number of levels.

B. *Reduced Order Modeling*

With the purpose of reducing the order of the system, let us consider Fig. 7 and Fig. 8. They depict the equivalent circuits for a 2x MBC when $u = 1$, and $u = 0$. They correspond to Fig. 5 and Fig 6, respectively.

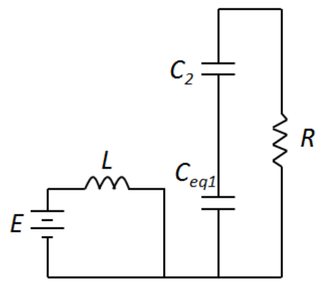

Fig. 7. Equivalent Circuit with u=1 and equivalent capacitances for the 2x MBC.

ISBN: 978-988-18210-0-3
ISSN: 2078-0958 (Print); ISSN: 2078-0966 (Online)

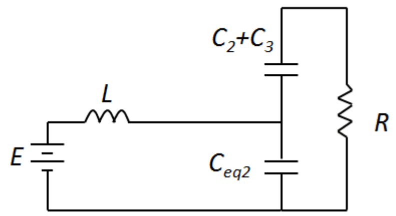

Fig. 8. Equivalent Circuit with u=0 and equivalent capacitances for the 2x MBC.

By employing basic principles and setting $C = C_1 = C_2 = C_3$, the equivalent capacitors become $C_{eq1} = 2C$ and $C_{eq2} = C$. In addition, the voltage across each capacitor at the output will be considered as the output voltage divided by the number of levels at the output (V/N). This assumption is supported by the voltage balancing feature of the MBC. In terms of equations we have

$$V_1 \cong V_2 \cong \frac{V}{2} \tag{10}$$

where V denotes the output voltage. If there is any number of levels we may write

$$V_1 \cong V_2 \cong V_3 \cong \cdots \cong V_N \cong \frac{V}{N} \tag{11}$$

Employing the equivalent circuit shown in Fig. 7 and using equation (11) the dynamics for inductor current and the output voltage can be written as

$$L\frac{d}{dt}i = E \tag{12}$$

$$C_{eq1}\frac{d}{dt}V = -\frac{N}{R}V \tag{13}$$

It is clear that expressions (12)-(13) are valid when the switch is closed. On the other hand, based on the equivalent circuit in Fig. 8 and using equation (11), the dynamics of the system is defined as

$$L\frac{d}{dt}i = -\frac{V}{N} + E \tag{14}$$

$$C_{eq2}\frac{d}{dt}V = i - \frac{N}{R}V \tag{15}$$

Equations (14)-(15) are valid when the switch is opened. Expressions (12)-(15) may be written into a more compact form that is valid for both commutation states $u = \{1,0\}$. This is

$$L\frac{d}{dt}i = -(1-u)\frac{V}{N} + E \tag{16}$$

$$[C_{eq1}u + (1-u)C_{eq2}]\frac{d}{dt}V = (1-u)i - \frac{N}{R}V \tag{17}$$

Average models are frequently employed for defining average feedback control laws in power electronics converters [11]. These models represent average currents and voltages. From equations (16) and (17) and considering u_{av} as the average input, we may write

$$L\frac{d}{dt}i = -(1-u_{av})\frac{V}{N} + E \tag{18}$$

$$[C_{eq1}u_{av} + (1-u_{av})C_{eq2}]\frac{d}{dt}V = (1-u_{av})i - \frac{N}{R}V \tag{19}$$

where the average input denoted by u_{av} is actually the duty cycle of the switch. Let us denote the inductor current i as x_1, the output voltage V as x_2 and $C_{eq1}u_{av} + (1-u_{av})C_{eq2}$ as $C(t)$. This capacitance denoted by $C(t)$ may be considered as a time-varying parameter. Equations (18) and (19) now become

$$L\frac{d}{dt}x_1 = -\frac{x_2}{N} + \frac{x_2}{N}u_{av} + E \tag{20}$$

$$C(t)\frac{d}{dt}x_2 = x_1 - x_1u_{av} - \frac{Nx_2}{R} \tag{21}$$

Using equations (20) and (21) and employing the inductor current as the output to be controlled, the reduced order nonlinear dynamic model for the MBC may be expressed as

$$\frac{d}{dt}x = f(x) + g(x)u_{av}$$

$$y = h(x) \tag{22}$$

where

$$f(x) = \begin{bmatrix} -\frac{x_2}{NL} + \frac{E}{L} \\ \frac{x_1}{C(t)} - \frac{Nx_2}{RC(t)} \end{bmatrix}; \;\; g(x) = \begin{bmatrix} \frac{x_2}{NL} \\ -\frac{x_1}{C(t)} \end{bmatrix}$$

$$h(x) = x_1; \quad x = [x_1 \quad x_2]^T$$

Equation (22) represents the reduced order average nonlinear dynamic model for the Nx MBC containing an arbitrary number of levels.

Figures 9 and 10 show the comparison between the full order model and the reduced order model. These simulations are performed for the 2x MBC.

The simulation of the full order model is carried out using the Synopsys Saber software and employing the electrical diagram of the 2x MBC, while the simulation of the reduced order model is obtained by using the MATLAB software to solve equation (22). The parameters involved in this simulation are $L = 250\mu H$, $C = C_1 = C_2 = C_3 = 220\mu F$, $N = 2$, $E = 40$, $R = 50$, and $u_{av} = 0.6$.

ISBN: 978-988-18210-0-3
ISSN: 2078-0958 (Print); ISSN: 2078-0966 (Online)

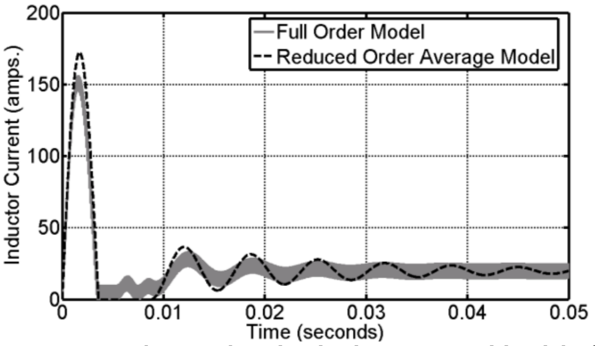

Fig. 9. Comparison between the reduced order average model and the full order model for the 2x MBC.

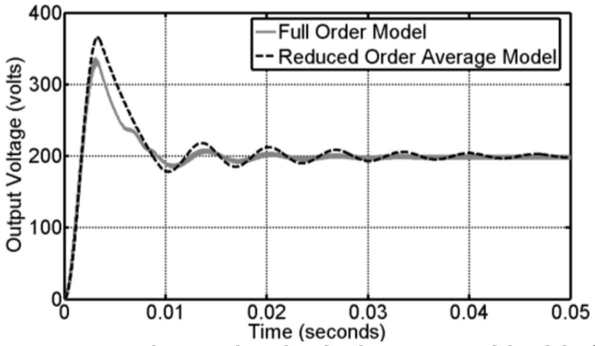

Fig. 10. Comparison between the reduced order average model and the full order model for the 2x MBC.

IV. Control Law

In this section, a controller based on the input-output feedback linearization theory [13] is defined for a MBC having an arbitrary number of levels *N*. This controller is derived by utilizing the reduced order model in (22) .

Employing the input-output feedback linearization technique, the following input can be considered

$$u_{av} = \frac{1}{L_g L_f^{r-1} h(x)} \left[-L_f^r h(x) + v \right]$$

Where r is the relative degree of the system [13], and it is obtained from

$$L_g L_f^{i-1} h(x) = 0;\ i = 1,2,\dots,r-1.$$

$$L_g L_f^{r-1} h(x) \neq 0$$

since

$$L_g\, h(x) = \frac{\partial h(x)}{\partial x} g(x) = [1 \quad 0] \begin{bmatrix} \frac{x_2}{NL} \\ -\frac{x_1}{C(t)} \end{bmatrix} = \frac{x_2}{NL} \neq 0$$

system in (22) has a relative degree equal to 1 providing that $x_2 \neq 0$. Therefore, the input may be written as [13]

$$u_{av} = \frac{v - L_f h(x)}{L_g h(x)} \tag{23}$$

where

$$L_f\, h(x) = \frac{\partial h(x)}{\partial x} f(x) = -\frac{x_2}{NL} + \frac{E}{L}$$

$$L_g\, h(x) = \frac{\partial h(x)}{\partial x} g(x) = \frac{x_2}{NL}$$

By substituting the input (23) into (22), the state equation corresponding to the inductor current x_1 is transformed into a linear form, this is

$$\frac{d}{dt} x_1 = v \tag{24}$$

In addition, parametric uncertainty will be addressed by using an integrator, this is

$$\frac{d}{dt} x_I = x_1 - i_{ref} \tag{25}$$

Then, a standard state feedback for the linear subsystem composed by (24)-(25) is defined as follow

$$v = -k_1 x_I - k_2 x_1 \tag{26}$$

In this particular case, the poles of the linear subsystem were proposed by considering a desired time constant for the closed loop system. The proposed poles are

$$s_{1,2} = [-1500 \quad -1501]$$

Employing the pole placement technique [11], the following gains are calculated

$$[k_1 \quad k_2] = [2.2515x10^6 \quad 3001]$$

It is clear that the stability of the equilibrium point associated with the subsystem defined by (24) and (25) is guaranteed by selecting adequate gains of the standard linear state feedback in (26). On the other hand, the stability of the equilibrium point of the subsystem defined by the second state equation in (22) may be verified by analyzing the zero dynamics of that subsystem [13].

In order to analyze the zero dynamics, let us assume that $v = 0$ and $x_1(0) = i_{ref} = 0$. Under these conditions, it is clear that $x_1(t) = 0$ for all *t*. The input u_{av} can be rewritten now as

$$u_{av} = \frac{-L_f h(x)}{L_g h(x)} = \frac{\frac{x_2}{NL} - \frac{E}{L}}{\frac{x_2}{NL}} \tag{27}$$

Considering $x_1(t) = 0$ and using (27), the second equation in (22) now becomes

$$\frac{d}{dt} x_2 = -\frac{N x_2}{RC(t)} \tag{28}$$

ISBN: 978-988-18210-0-3
ISSN: 2078-0958 (Print); ISSN: 2078-0966 (Online)

Let us consider the following Lyapunov function

$$V(x_2) = \frac{1}{2}x_2^2$$

its derivative is given by

$$\dot{V}(x_2) = x_2\left(-\frac{Nx_2}{RC(t)}\right) = -\frac{Nx_2^2}{RC(t)}$$

On the other hand, substituting C_{eq1} and C_{eq2} into the expression for $C(t)$, we obtain

$$C(t) = Cu_{av} + C$$

From a practical standpoint, the duty cycle is defined in the range (0,1). This is $0 < u_{av} < 1$. Therefore $C(t) > 0$. Since parameters N, R and $C(t)$ are strictly positive, the derivative $\dot{V}(x_2)$ is negative definite. Therefore the zero dynamics of the MBC is stable at $x_2 = i_{ref}$.

V. Experimental Results

As it was established earlier, the output voltage is indirectly controlled by defining a reference for the inductor current in terms of the desired output voltage. The expression that relates both variables is derived by carrying out a steady state analysis of the dynamic model in (22), i.e.

$$i_{ref} = \frac{V_{ref}^2}{RE} \tag{29}$$

where V_{ref} denotes the desired output voltage.

The implementation of the control law is carried out by employing RTAI-Lab [14] as a Linux based real-time platform and a NI PCI-6024E data acquisition board.

Fig. 11 depicts the Linux-based real time program of the implemented controller.

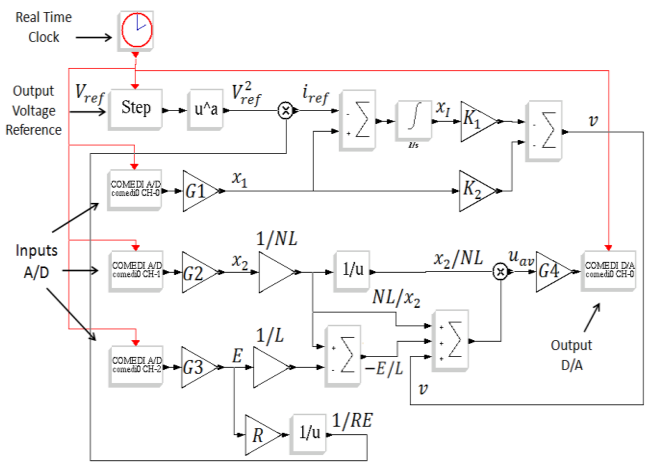

Fig. 11. Real time program of the implemented controller in RTAI-Lab.

The parameters involved in the implementation are: $L = 250\mu H$, $C = C_1 = C_2 = C_3 = 222.2\mu F$, $N = 2$, $E = 30$, $R = 230$ and $V_{ref} = 150V$. Figure 12 shows the experimental and simulated traces of the output voltage.

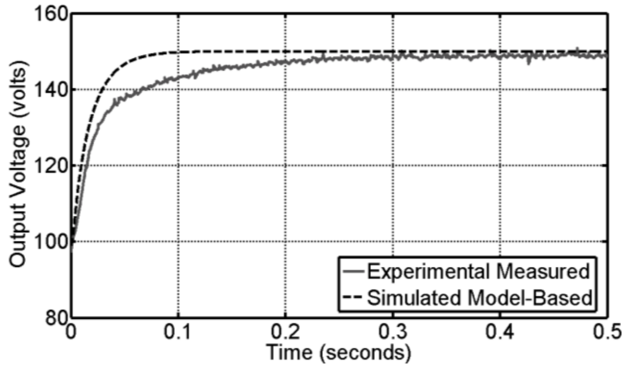

Fig. 12. Transient traces of the experimental measured and simulated model-based output voltage.

It is important to note that since power losses in some electronic devices (diodes, transistor) are not included in the model defined by (22), the actual experimental measured output voltage is slightly smaller than the desired one.

Another experiment was designed for the purpose of testing the closed loop system in more demanding conditions. In the previous test the input voltage E is constant. In this new test, the input voltage E is varied as it is shown in Fig. 13. According to expression (29) the set point for the inductor current i_{ref} is calculated (in real time) as the input voltage E is varied. Figure 14 shows the experimental measured inductor current. The resulting experimental measured output voltage is depicted in Figure 15.

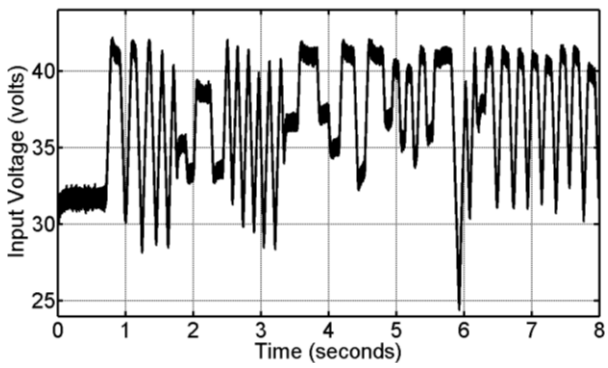

Fig. 13. Experimental input voltage E.

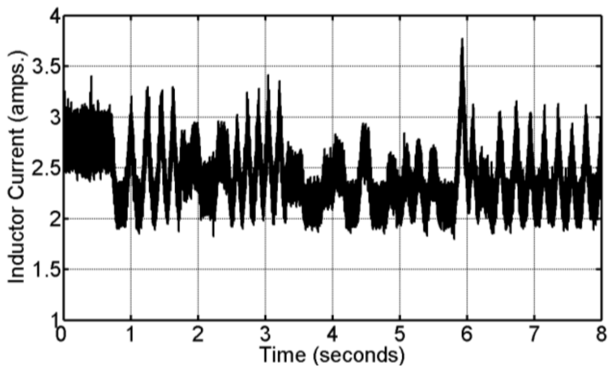

Fig. 14. Experimental inductor current when variations of the input voltage appear.

VI. Conclusion

This paper presents the state space modeling of a DC-DC Multilevel Boost Converter. Full and reduced order nonlinear models for the MBC are proposed. A second order

ISBN: 978-988-18210-0-3
ISSN: 2078-0958 (Print); ISSN: 2078-0966 (Online)

model is able to define an approximate dynamics for the MBC having any number of levels. A good agreement is obtained when comparing the full order and the reduced order models. In addition, the output voltage is indirectly controlled by using a control law based on the input-output feedback linearization technique. The controller is derived using the reduced order model of the MBC. Excellent experimental results are shown for a 2x MBC. In future works, a controller for the MBC having higher number of levels will be implemented by using the reduced order model derived in this paper.

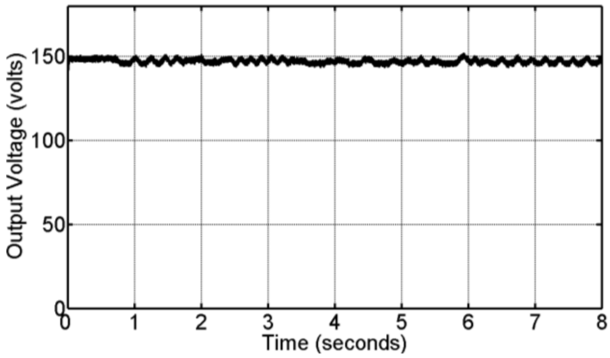

Fig. 15. Experimental measured output voltage when variations of the input voltage appear.

REFERENCES

[1] R. D. Middlebrook, "Transformerless DC-to-DC converters with large conversion ratios." *IEEE Trans. Power Electronics*, vol. 3, Issue 4, pp. 484-488. Oct. 1988.

[2] D. Maksimovic; S. Cuk, "Switching converters with wide DC conversion range." *IEEE Trans. Power Electronics,* vol. 6, Issue 1, pp. 151-157. Jan. 1991.

[3] B. Axelrod; Y. Berkovich, A. Ioinovici, "Switched-Capacitor/Switched-Inductor Structures for Getting Transformerless Hybrid DC–DC PWM Converters." *IEEE Trans. Circuits and Systems I*, vol. 55, Issue 2, pp. 687-696, March 2008.

[4] Zhou Dongyan, A. Pietkiewicz, S. Cuk, *"A three-switch high-voltage converter."* IEEE Transactions on Power Electronics, Volume 14, Issue 1, Jan. 1999 Page(s):177 – 183.

[5] Leyva-Ramos, J.; Ortiz-Lopez, M.G.; Diaz-Saldierna, L.H.; Morales-Saldana, J.A. "Switching regulator using a quadratic boost converter for wide DC conversion ratios." *IET Power Electronics*. vol. 2, Issue 5, pp. 605-613, Sept. 2009.

[6] Rosas-Caro, J.C.; Ramirez, J.M.; Peng, F.Z.; Valderrabano, A.; , "A DC-DC multilevel boost converter," *Power Electronics, IET* , vol.3, no.1, pp.129-137, January 2010.

[7] Rosas-Caro, J.C.; Ramirez, J.M.; Garcia-Vite, P.M.; , "Novel DC-DC Multilevel Boost Converter," Power Electronics Specialists Conference, 2008. PESC 2008. IEEE , vol., no., pp.2146-2151, 15-19 June 2008.

[8] Rosas-Caro, J.C.; Ramirez, J.M.; Valderrabano, A.; , "Voltage balancing in DC/DC multilevel boost converters," Power Symposium, 2008. NAPS '08. 40th North American , vol., no., pp.1-7, 28-30 Sept. 2008.

[9] Morales-Saldana, J.A.; Galarza-Quirino, R.; Leyva-Ramos, J.; Carbajal-Gutierrez, E.E.; Ortiz-Lopez, M.G.; , "Multiloop controller design for a quadratic boost converter," *Electric Power Applications, IET* , vol.1, no.3, pp.362-367, May 2007.

[10] Bo Yin; Oruganti, R.; Panda, S.K.; Bhat, A.K.S.; , "A Simple Single-Input–Single-Output (SISO) Model for a Three-Phase PWM Rectifier," *Power Electronics, IEEE Transactions on* , vol.24, no.3, pp.620-631, March 2009.

[11] Hebertt Sira-Ramírez and Ramón Silva-Ortigoza. "*Control Design Techniques in Power Electronics Devices*." *Springer*. 2006.

[12] Gensior, A.; Sira-Ramirez, H.; Rudolph, J.; Guldner, H.; , "On Some Nonlinear Current Controllers for Three-Phase Boost Rectifiers," *Industrial Electronics, IEEE Transactions on* , vol.56, no.2, pp.360-370, Feb. 2009.

[13] A. Isidori. *Nonlinear Control Systems*. Springer, 3rd edition, 1995.

[14] R. Bucher, S. Mannori and T. Netter. *RTAI-Lab tutorial: Scilab, Comedi and real-time control*. 2008.

ISBN: 978-988-18210-0-3
ISSN: 2078-0958 (Print); ISSN: 2078-0966 (Online)